Figure S1

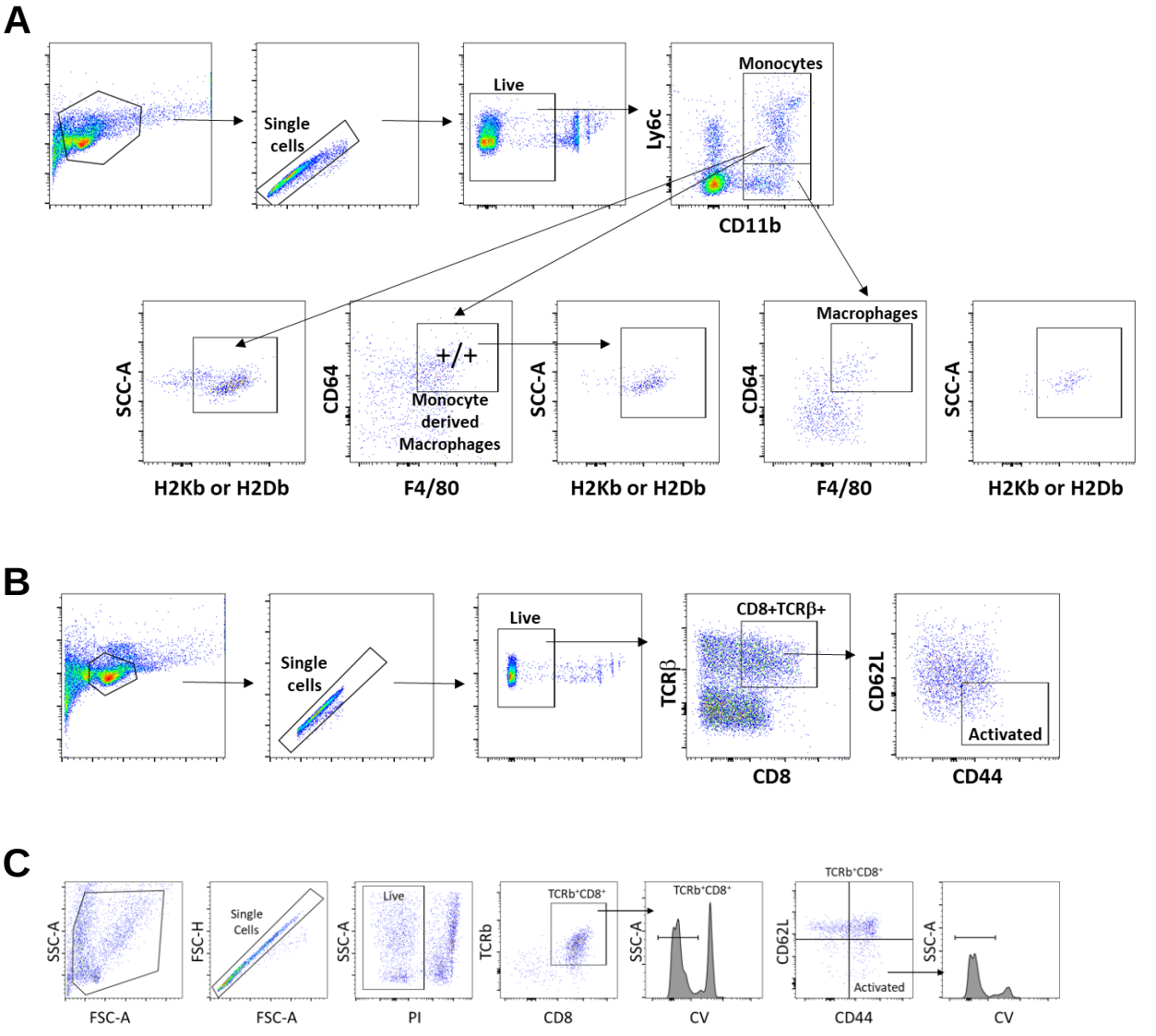
A
Single cells
Live
Monocytes
Ly6c
CD11b
SCC-A
H2Kb or H2Db
CD64
+/+
Monocyte derived Macrophages
F4/80
SCC-A
H2Kb or H2Db
Macrophages
CD64
F4/80
SCC-A
H2Kb or H2Db
B
Single cells
Live
CD8+TCRβ+
TCRβ
CD8
CD62L
Activated
CD44
C
SSC-A
FSC-A
FSC-H
Single Cells
FSC-A
SSC-A
Live
PI
TCRb
TCRb+CD8+
CD8
SSC-A
TCRb+CD8+
CV
CD62L
TCRb+CD8+
Activated
CD44
SSC-A
CV

Figure. S1. Flow cytometry gating strategies. (A) Myeloid cell flow gating strategies. **(B)** T cell flow gating strategies. **(C)** T cell flow gating strategies for T cell activation assays.

Figure S2

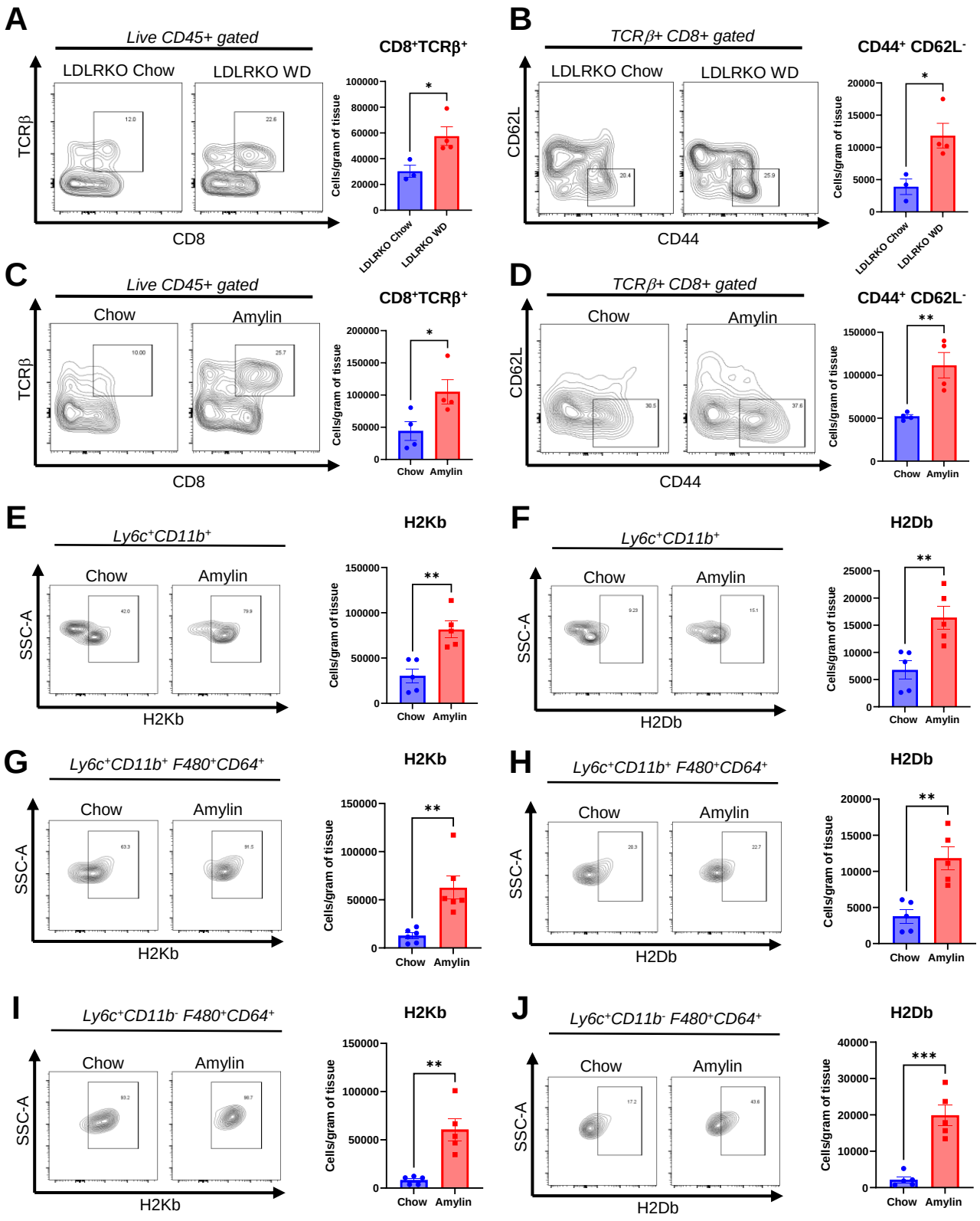
A
Live CD45+ gated
LDLRKO Chow
LDLRKO WD
TCRβ
CD8
CD8+TCRβ+
Cells/gram of tissue
B
TCRβ+ CD8+ gated
CD62L
CD44
CD44+ CD62L-
C
Chow
Amylin
D
E
Ly6c+CD11b+
SSC-A
H2Kb
H2Db
F
G
Ly6c+CD11b+ F480+CD64+
H
I
Ly6c+CD11b- F480+CD64+
J

Figure. S2. $CD8^+$ T cells are upregulated in NASH with increased H2Kb and H2Db in myeloid cells. LDLRKO mice on chow or WD for 12 wks (n=3-4 mice per group, 2 replicate studies) (A-B). Taconic mice on chow or amylin diet for 28 wks (n=5 mice per group, 2 replicate studies) (C-D). WT amylin mice on diet for 28 wks (n=4, 2 replicate studies) (E-J). Flow analysis of *$CD8^+$ $TCRb^+$* cells **(A,C)** and activation (*$CD44^+CD62L^-$*) **(B,D).** Representative flow plots of monocyte H2Kb **(E)** and H2Db **(F)** expression. Representative flow plots of monocyte derived macrophage H2Kb **(G)** and H2Db **(H)** expression. Representative flow plots of macrophage H2Kb **(I)** and H2Db **(J)** expression. Data shown as the mean ± SEM. Two-tailed unpaired Student's t-tests was performed and considered statistically significant for $P<0.05$ (*), $P<0.01$ (**), and $P<0.001$(***).

Figure S3

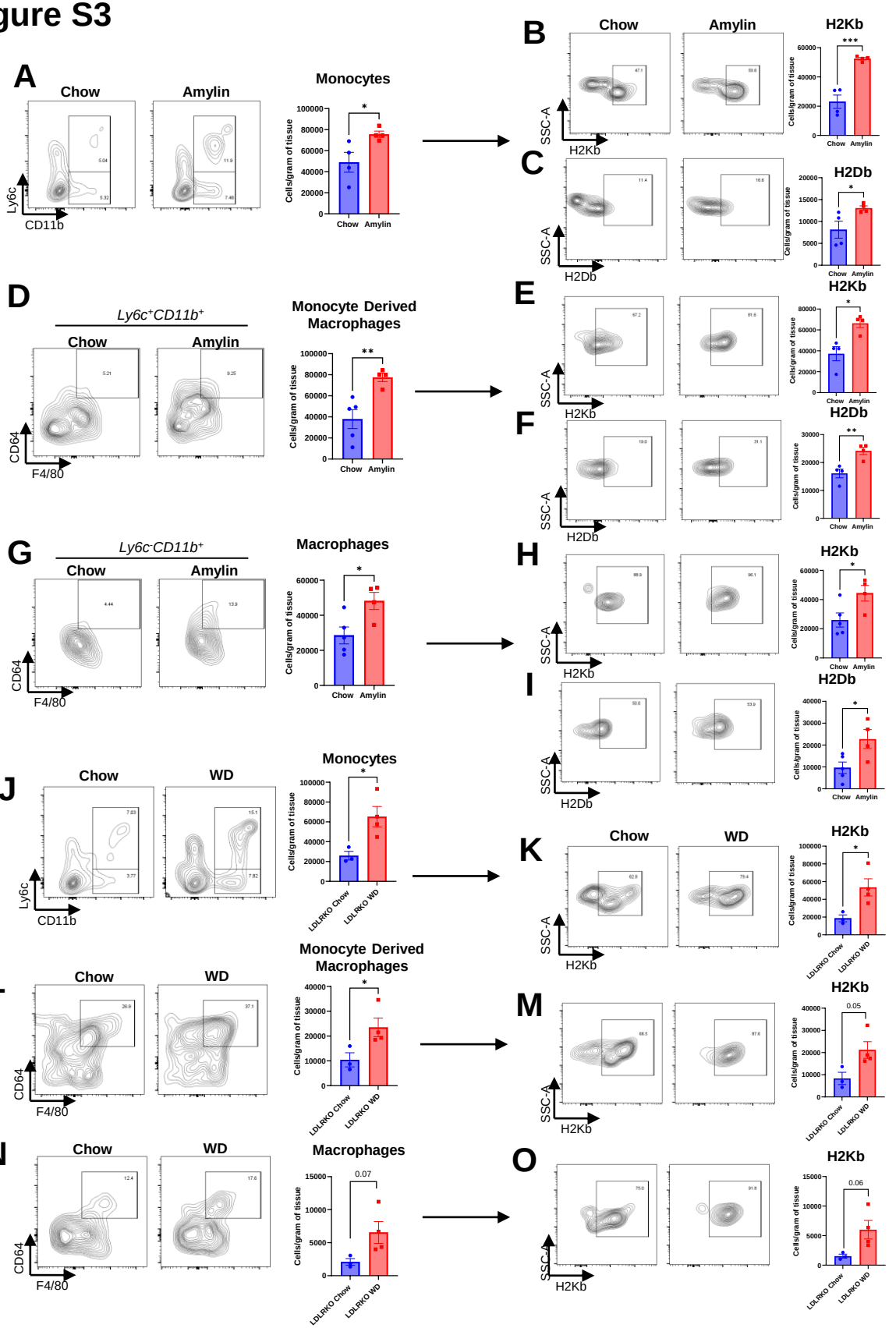
A
Chow
Amylin
Ly6c
CD11b
Monocytes
Cells/gram of tissue
Chow
Amylin
B
H2Kb
SSC-A
C
H2Db
D
Ly6c+CD11b+
CD64
F4/80
Monocyte Derived Macrophages
E
F
G
Ly6c-CD11b+
Macrophages
H
I
J
WD
LDLRKO Chow
LDLRKO WD
K
L
M
N
O
0.05
0.07
0.06

Figure. S3. H2Kb and H2Db expression is upregulated in NASH myeloid cells. Taconic mice on chow or amylin diet for 28 wks (n=4 mice per group, 2 replicate cohorts) **(A-I)**. LDLRKO mice on chow or WD for 12 wks (n = 3-4 mice per group, 1 cohort) **(J-O)**. Taconic model flow analysis of monocytes (*Ly6c*$^{+}$*CD11b*$^{+}$) **(A),** monocyte H2Kb expression **(B)**, and monocyte H2Db expression **(C)**. Flow analysis of monocyte derived macrophages (*Ly6c*$^{+}$*CD11b*$^{+}$*CD64*$^{+}$*F480*$^{+}$) **(D),** monocyte derived macrophage H2Kb expression **(E)**, and monocyte derived macrophage H2Db expression **(F)**. Flow analysis of macrophages (*Ly6c*$^{-}$*CD11b*$^{+}$*CD64*$^{+}$*F480*$^{+}$) **(G),** macrophages H2Kb expression **(H)**, and macrophages H2Db expression **(I)**. LDLRKO model flow analysis of monocytes (*Ly6c*$^{+}$*CD11b*$^{+}$) **(J)** and monocyte H2Kb expression **(K)**. Flow analysis of monocyte derived macrophages (*Ly6c*$^{+}$*CD11b*$^{+}$*CD64*$^{+}$*F480*$^{+}$) **(L)** and monocyte derived macrophage H2Kb expression **(M)**. Flow analysis of macrophages (*Ly6c*$^{-}$*CD11b*$^{+}$*CD64*$^{+}$*F480*$^{+}$) **(N)** and macrophages H2Kb expression **(O).** Data shown as the mean ± SEM. Two-tailed unpaired Student's t-tests was performed and considered statistically significant for $P<0.05$ (*), $P<0.01$ (**), and $P<0.001$(***).

Figure S4

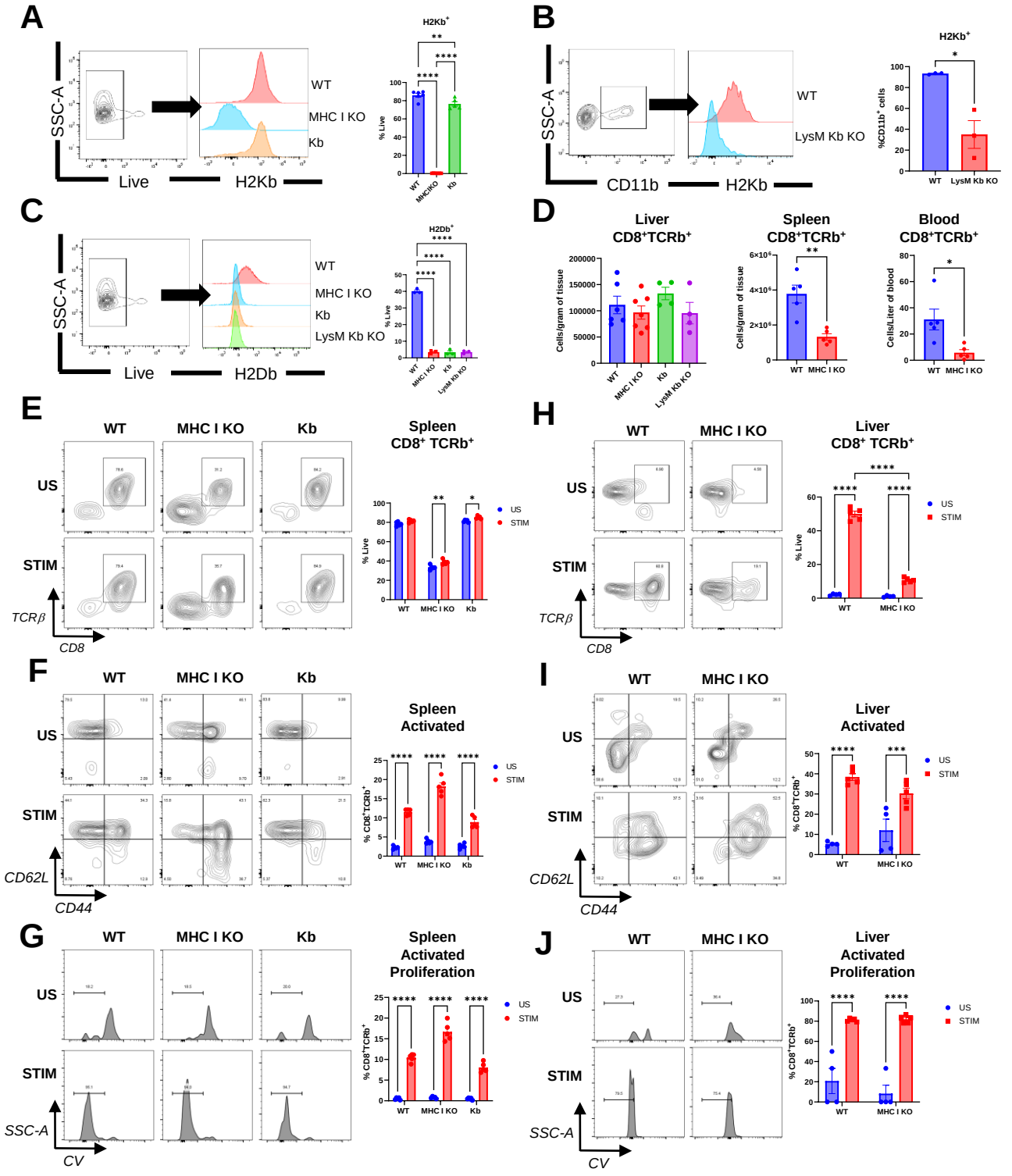
A
SSC-A
Live
H2Kb
WT
MHC I KO
Kb
H2Kb+
% Live
B
SSC-A
CD11b
H2Kb
WT
LysM Kb KO
H2Kb+
%CD11b+ cells
C
SSC-A
Live
H2Db
WT
MHC I KO
Kb
LysM Kb KO
H2Db+
% Live
D
Liver CD8+TCRb+
Spleen CD8+TCRb+
Blood CD8+TCRb+
Cells/gram of tissue
Cells/Liter of blood
WT
MHC I KO
Kb
LysM Kb KO
E
WT
MHC I KO
Kb
US
STIM
TCRβ
CD8
Spleen CD8+ TCRb+
% Live
H
Liver CD8+ TCRb+
F
Spleen Activated
% CD8+TCRb+
CD62L
CD44
I
Liver Activated
G
Spleen Activated Proliferation
SSC-A
CV
J
Liver Activated Proliferation

Figure. S4. Efficient H2Kb and H2Db knockout in MHC I KO, Kb transgenic mice, and Kb KO in myeloid cells with functional spleen CD8$^+$ T cells. WT, MHC I KO, Kb, LysM Kb KO chow mice (n=5-7 per group, three cohorts). Representative flow plots of isolated liver cells gated for: **(A)** total H2Kb$^+$ cells, **(B)** CD11b$^+$ cells H2Kb$^+$ expression, and **(C)** total H2Db$^+$ cells. **(D)** Flow cytometry data for CD8$^+$TCRb$^+$ cells in WT, MHC I KO, Kb, and LysM Kb KO chow mouse livers. T cell activation assay with sorted CD8$^+$ splenic T cells under stimulated and unstimulated conditions from WT, MHC I KO, and Kb mice harvested after 3 days (n=5, in triplicate). Flow cytometry analysis of CD8$^+$TCRb$^+$ cells **(E),** activation (CD44$^+$, CD62L$^-$) **(F),** and proliferation **(G).** T cell activation assay with sorted CD8$^+$ Liver T cells under stimulated and unstimulated conditions from WT or MHC I KO chow mice harvested after 3 days (n=4-5). Flow cytometry analysis of CD8$^+$TCRb$^+$ cells **(H),** activation (CD44$^+$, CD62L$^-$) **(I),** and proliferation **(J).** Data shown as the mean ± SEM. Two-tailed unpaired Student's t-tests for data with two groups and Two-way ANOVA was performed for more than two and was considered statistically significant for $P<0.05$ (*), $P<0.01$ (**), $P<0.001$(***), and $P<0.0001$(****).

Figure S5

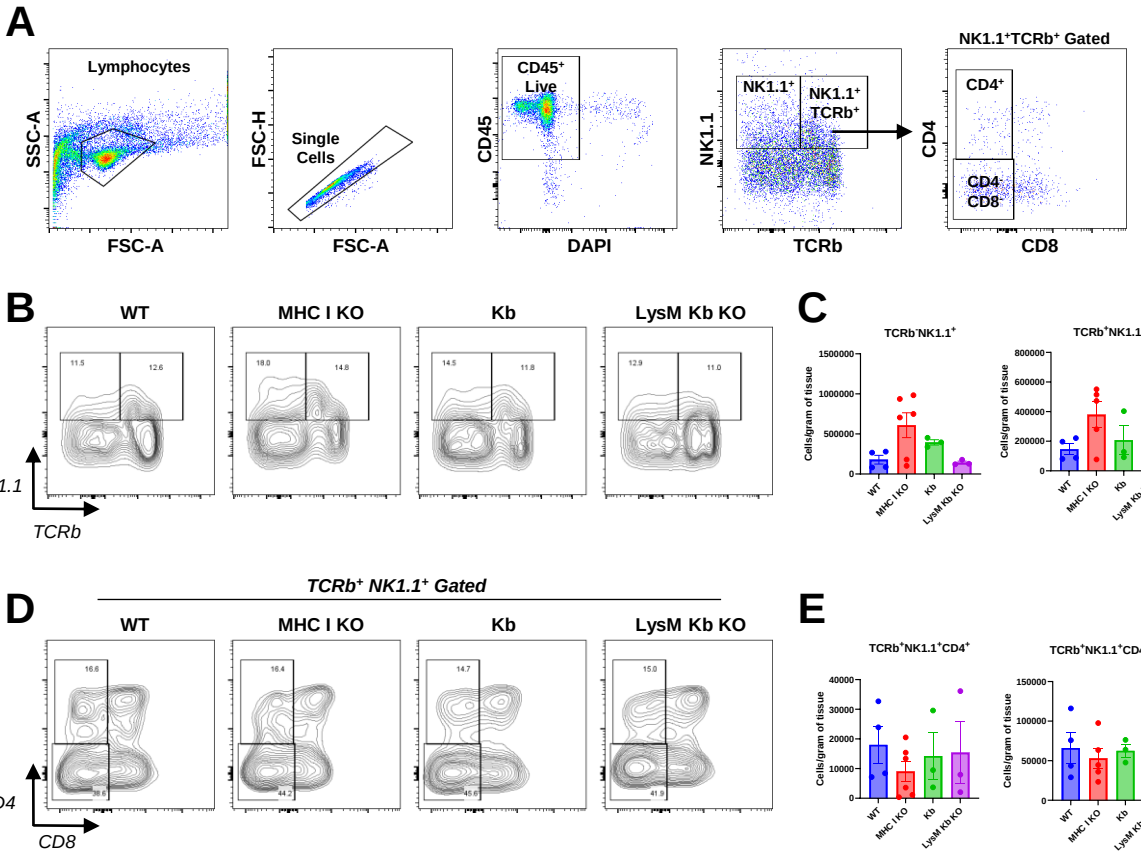
A
Lymphocytes
SSC-A
FSC-A
Single Cells
FSC-H
FSC-A
CD45+ Live
CD45
DAPI
NK1.1+
NK1.1+ TCRb+
NK1.1
TCRb
NK1.1+TCRb+ Gated
CD4+
CD4- CD8-
CD4
CD8
B
WT
MHC I KO
Kb
LysM Kb KO
11.5
12.6
18.0
14.8
14.5
11.8
12.9
11.0
NK1.1
TCRb
C
TCRb-NK1.1+
TCRb+NK1.1+
Cells/gram of tissue
1500000
1000000
500000
0
800000
600000
400000
200000
WT
MHC I KO
Kb
LysM Kb KO
D
TCRb+ NK1.1+ Gated
WT
MHC I KO
Kb
LysM Kb KO
16.6
16.4
14.7
15.0
CD4
CD8
E
TCRb+NK1.1+CD4+
TCRb+NK1.1+CD4-CD8-
Cells/gram of tissue
40000
30000
20000
10000
0
150000
100000
50000
WT
MHC I KO
Kb
LysM Kb KO

Figure. S5. NK1.1+ and NK T cells are not impacted in livers of MHC I KO, Kb, or LysM Kb KO mice. Female WT, MHC I KO, Kb, and LysM Kb KO chow mice (n=3-6 per group). **(A)** Representative flow gating strategy for NK T cells. **(B-C)** Flow analysis of *NK1.1*$^{+}$ *TCRb*$^{+}$ and *NK1.1*$^{+}$ *TCRb*$^{-}$ cells. **(D-E)** Flow analysis of *CD4*$^{+}$ *or CD4*$^{-}$*CD8*$^{-}$ expression in *NK1.1*$^{+}$ *TCRb*$^{+}$ cells. Data shown as the mean ± SEM. One-Way ANOVA was performed.

Figure S6

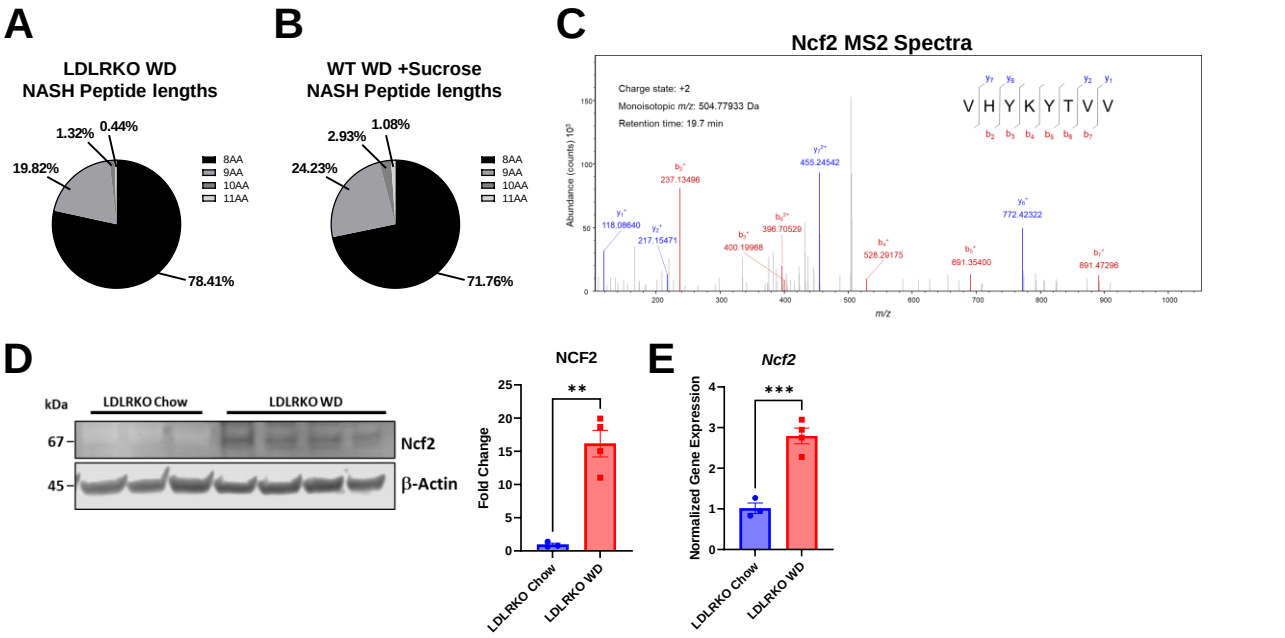
A
LDLRKO WD
NASH Peptide lengths
1.32%
0.44%
19.82%
78.41%
8AA
9AA
10AA
11AA
B
WT WD +Sucrose
NASH Peptide lengths
2.93%
1.08%
24.23%
71.76%
8AA
9AA
10AA
11AA
C
Ncf2 MS2 Spectra
Charge state: +2
Monoisotopic m/z: 504.77933 Da
Retention time: 19.7 min
V H Y K Y T V V
Abundance (counts) 10³
m/z
237.13496
455.24542
118.08640
217.15471
396.70529
400.19968
528.29175
691.35400
772.42322
891.47296
D
kDa
LDLRKO Chow
LDLRKO WD
67
45
Ncf2
β-Actin
NCF2
Fold Change
**
LDLRKO Chow
LDLRKO WD
E
Ncf2
Normalized Gene Expression
***
LDLRKO Chow
LDLRKO WD

Figure. S6. NASH Peptide characterization. LDLRKO mice on WD for 12 wks (n = 3-4 mice per group, 2 replicate cohorts). WT mice on chow or WD and sucrose water for 25 wks (n=5 mice per group, one cohort). **(A)** Unique NASH peptide lengths from LDLRKO NASH model **(A)** and WT NASH model **(B)**. **(C)** LC-MS/MS MS2 Ncf2 spectrum. Total liver Ncf2 protein **(D)** and gene **(E)** expression from LDLRKO NASH model. Data shown as the mean ± SEM. Two-tailed unpaired Student's t-tests was performed and considered statistically significant for $P<0.01$ (**) and $P<0.001$(***).

Figure S7

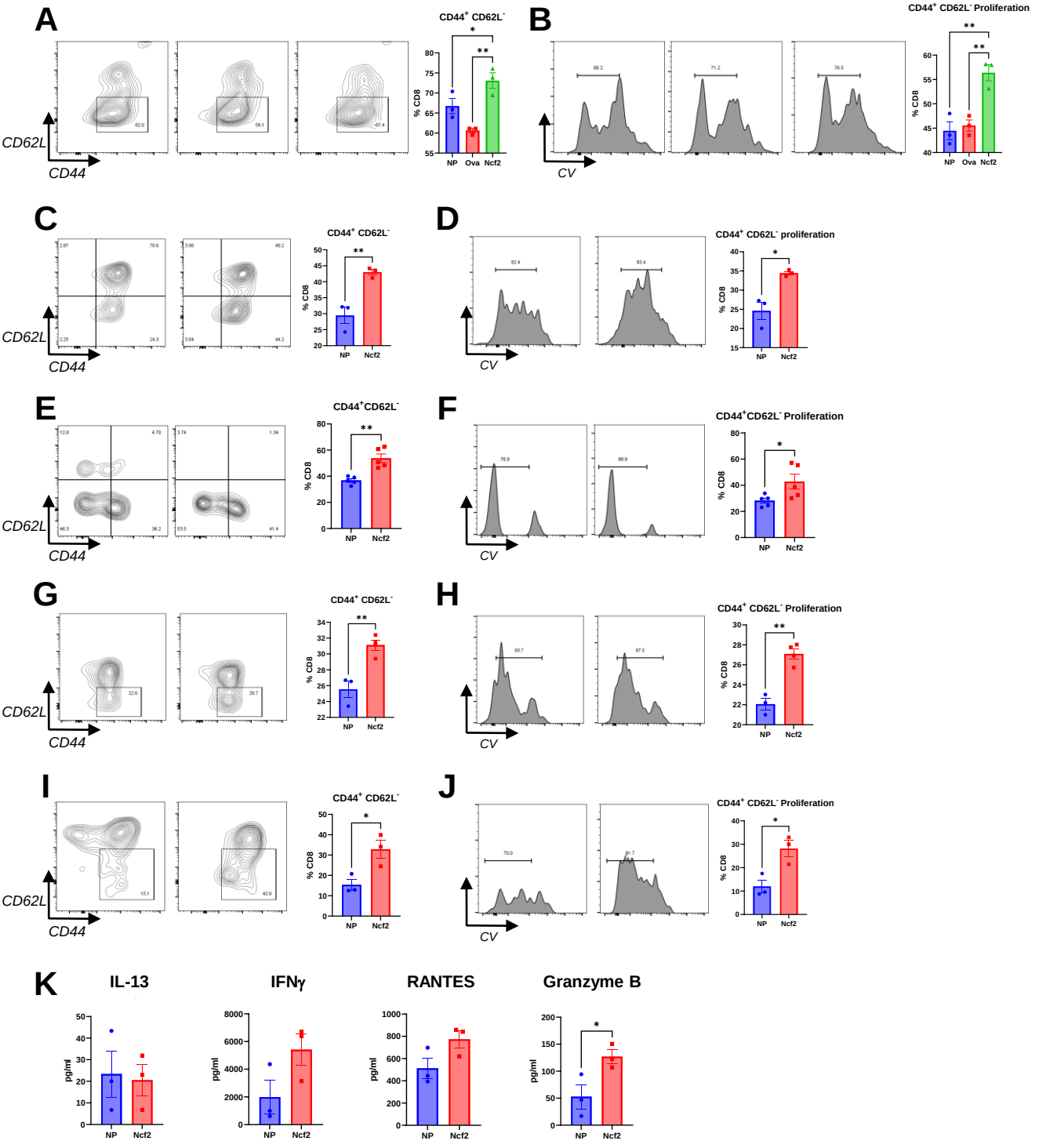
A
CD62L
CD44
CD44+ CD62L-
% CD8
NP
Ova
Ncf2
B
CV
CD44+ CD62L- Proliferation
C
CD44+ CD62L-
D
CD44+ CD62L- proliferation
E
CD44+CD62L-
F
CD44+CD62L- Proliferation
G
CD44+ CD62L-
H
CD44+ CD62L- Proliferation
I
CD44+ CD62L-
J
CD44+ CD62L- Proliferation
K
IL-13
IFNγ
RANTES
Granzyme B
pg/ml

Figure. S7. Ncf2 peptide activates hepatic $CD8^+$ T cells and splenic $CD8^+$ T cells in various models of NASH. $CD8^+$ T cells were isolated from livers or spleens of Tac NASH, LDLRKO NASH, or WT NASH models (n = 2 mice combined per trial) done in 3-4 replicate studies and cocultured with NP, Ova, or Ncf2 pulsed RMA-S cells. Flow analysis of hepatic $CD8^+$ T cell activation **(A)** and proliferation **(B)** in the Tac NASH model after 3 days incubation with peptide pulsed RMA-S cells under stimulated (CD3/CD28) conditions. Flow analysis of splenic $CD8^+$ T cell activation **(C)** and proliferation **(D)** in the Tac NASH model after 5 days incubation with peptide pulsed RMA-S cells under stimulated conditions. Flow analysis of splenic $CD8^+$ T cell activation **(E)** and proliferation **(F)** in the Tac NASH model after 5 days incubation with peptide pulsed RMA-S cells under unstimulated conditions supplemented with 100ng/ml IL-2. Flow analysis of splenic $CD8^+$ T cell activation **(G)** and proliferation **(H)** in the WT NASH model after 5 days incubation with peptide pulsed RMA-S cells. Flow analysis of splenic $CD8^+$ T cell activation **(I)** and proliferation **(J)** in the LDLRKO NASH model after 5 days incubation with peptide pulsed RMA-S cells. **(K)** Cytokine analysis of media from splenic $CD8^+$ T cells incubated with Ncf2 peptide pulsed RMA-S cells in the LDLKO NASH model. Data shown as the mean ± SEM. Two-tailed unpaired Student's t-tests was performed for data sets with 2 groups and Two-way ANOVA was performed for groups more than 2 and was considered statistically significant for $P<0.05$ (*) and $P<0.01$ (**).